Article

Simulated Effects of Sudden Increases in Electromagnetic Activity on Deviations in Random Electron Tunnelling Behaviour Associated with Cognitive Intention

Joey M. Caswell[1,2], David A. E. Vares[1,3], Lyndon M. Juden-Kelly[1,2] & Michael A. Persinger[1,2,3,4 *]

Consciousness Research Laboratory [1], Behavioural Neuroscience [1], Human Development [2], Experimental Psychology [3], and Biomolecular Science [4] Programs, Laurentian University, Sudbury, Ontario, Canada P3E 2C6

ABSTRACT

Reliable evidence from the Jahn-Dunne studies conducted over several decades indicated that human proximity can affect the dynamics of certain processes that strongly depend upon "random" processes. Random Event Generators (REG) operate through "random" electron tunneling through spaces that are within the same order of magnitude as synapses. If the mechanisms by which these human-machine interactions occur involve electromagnetic processes, then application of specific temporally patterned magnetic fields to the human volume should affect the strength of the deviation from "random" variations. Whole-body exposure to ~400 nT, complex-patterned magnetic fields based upon 3 ms point durations reversed the effects of normal "intention" upon the operation of REGs. The energies generated within the cerebral volume by that field if emitted as irradiative power were within the range of the mass equivalent of an electron at the level of p-n junction of the semiconductor. These results support the hypothesis that "intention" can be affected experimentally and the energies within the vicinity of the actual dynamic space (~1 μm^2) of the p-n junction of the REG match the extended power of the magnetic energy contained within the cerebrum.

Key Words: Intention, Consciousness, p-n junctions; Random Event Generators (REG), Electromagnetic Fields

1. Introduction

As a species, our dependence on technology can no longer be understated. This reliance can cause the machine of society to grind to a halt as a result of power failures or other electrical disturbances. The study of space weather, particularly the geomagnetic field, has elucidated one mechanism by which both electrical and biological systems are affected on Earth by even small environmental electromagnetic variations. The convergence of a number of scientific disciplines, including geophysics, biology, environmental science, and engineering, have led to a number of discoveries regarding the effects of space weather on terrestrial systems, from human physiology and health to navigation and communications systems.

*Corresponding author: Michael A. Persinger E-mail: mpersinger@laurentian.ca

The same progression of discovery due to the integration of previously disparate fields of study has also proven fortuitous for the study of consciousness, parapsychology, and physical anomalies research. By extending the focus of investigation in these areas from theoretical models of psychology and philosophy to the search for biophysical relationships, mechanistic explanations based on physical principles have begun to emerge. These areas have recently flourished with new models involving physical quantification and interdisciplinary investigation bolstered by new technologies. This increasingly transdisciplinary engagement has encouraged the search for physical relationships which might reveal potential mechanisms by which anomalous or *non-local* interactions occur in association with psychobiological systems.

The inner core of the Earth, composed of iron-alloy and other lighter elements, rotates within the liquid iron outer core, and this rotation produces a magnetic field through a dynamo effect. This magnetic field extends outwards around the planet to reach solar winds and form the geomagnetic field. It may behave as a filter or transducer of extraterrestrial stimuli such as cosmic rays or protons. Geomagnetic activity and subsequent conditions within the planetary atmosphere affect terrestrial biology, including a number of species of birds [1], fish [2], and terrestrial mammals [3]. In the context of human studies, effects of geomagnetic activity have been identified for cardiovascular functioning [4], bioelectrical activity in the brain [5], and emotional state [6]. Geomagnetic storms typically occur in relation to solar activity including variations in solar wind velocity [7], dynamic pressure changes [8], and coronal mass ejections [9].

It has also been demonstrated that the random output of an external physical system is correlated with the conscious "intention" of a human operator [10-11]; decades of research have consistently documented the apparent phenomenon of consciousness-correlated collapse (3C), which suggests that the behaviour of non-deterministic systems may be affected by human consciousness. Given that the relationship between brain activity and variations in the Earth's geomagnetic field is well documented, and there have been potential associations revealed between the 3C phenomenon and cerebral effects [12-14], it is hypothesized that any potential temporal contiguity between the electromagnetic interactions associated with cognitive intention may be reflected in a relationship between a measure of 3C performance and environmental variations in electromagnetic activity.

The state of geomagnetic activity in particular has previously been studied in the specific context of anomalous physical phenomena associated with consciousness. For example, *passive* anomalous processes, such as remote viewing, were shown to exhibit a negative correlation between task accuracy and geomagnetic activity (GMA) [15]. The most powerful effects for both spontaneous and experimental forms of accessing information at a distance through non-conventional means occur when the global variations are within the 5 to 8 nT range. Slightly higher intensities are more likely to occur during precognitive dreams [16-17]. Alterations of the local geomagnetic field occur when an exceptional individual engaged in intuitive states similar to remote viewing phenomena [18-19]. The magnetic energy associated with decrease in geomagnetic intensity within the volume surrounding the person's cerebrum was the same order of magnitude as the increased photon power density recorded within this boundary.

Although studies have previously investigated the relationship between GMA and *active* anomalous physical processes, such as consciousness-correlated collapse (3C) of external

random systems, these tend to be relatively restricted in scope and subsequent analyses have failed to determine a potential effect of geomagnetism on external effects of conscious intention [20-21]. For example, it has been successfully determined that recurrent-spontaneous effects of consciousness on the local environment at the macro-scale tend to occur during periods of increased GMA [22-23]. Although a number of these experiences may be subject to relative interpretation, there is contemporary quantitative evidence suggesting the potential for thought to affect matter [24], as well as the relevant quantitative convergence which supports a link between micro- and macro-quantum processes associated with cortical activity [25].

That even small perturbations of ~20-40 nT have been shown to affect human neurophysiology [26] suggests that weak intensity electromagnetic fields (EMF) have the potential capacity to disrupt normal functioning of cognitive processes. While we have previously demonstrated that transcerebral application of a specific physiologically-patterned EMF shows a potential to increase the capacity to engage external effects of consciousness [13], we hypothesized that full-body exposure to a relatively 'noisy' signal not patterned after any specific physiological process would potentially disrupt the occurrence of the 3C phenomenon. We designed an experiment in which sudden increases in patterned, weak-intensity electromagnetic activity were simulated using a variation on protocols employed in our laboratory for previous experiments [27-28]. Participants attempted to influence the output of a random event generator (REG) device during both control and EMF conditions.

2. Methods

2.1. Subjects

Participant age ranged from 22-30 years for N = 8 (N = 3 females, N = 5 males). All were recruited from Laurentian University campus.

2.2. Equipment

Simulated EMF increases were produced using two large custom-built rectangular coils (1.15 x 1.15 m) placed 1 m apart on either side of the participant seating area, ~36 cm away from their bodies. The random event generator (REG) device was also placed within the area of the coils ~25 cm in front of the participant on his or her right side. The magnetic field was produced by a DOS PC system using custom software designed by Professor Stan Koren. The original waveform designed to imitate increased GMA consists of 5071 individual points. To simulate a sudden impulse the point durations were designed to be 69 ms. However, during the following experiment the same field pattern was presented with point durations of 3 msec each, and a 3 msec delay between each point, a significantly faster duration and presentation compared to simulation of natural geomagnetic increases [27]. The 3 ms point durations were selected on the bases of the enhanced physiological effectiveness. The value of each point in the waveform ranged between 0-256 and was converted to a voltage equivalent (-5 to +5 V) using a custom-built digital-to-analogue converter device which delivered the associated current through the coils. The overall intensity of the subsequent electromagnetic field produced by the system had a

peak intensity of ~400 to 500 nT as measured by power meters. The actual waveform image is displayed in Figure 1.

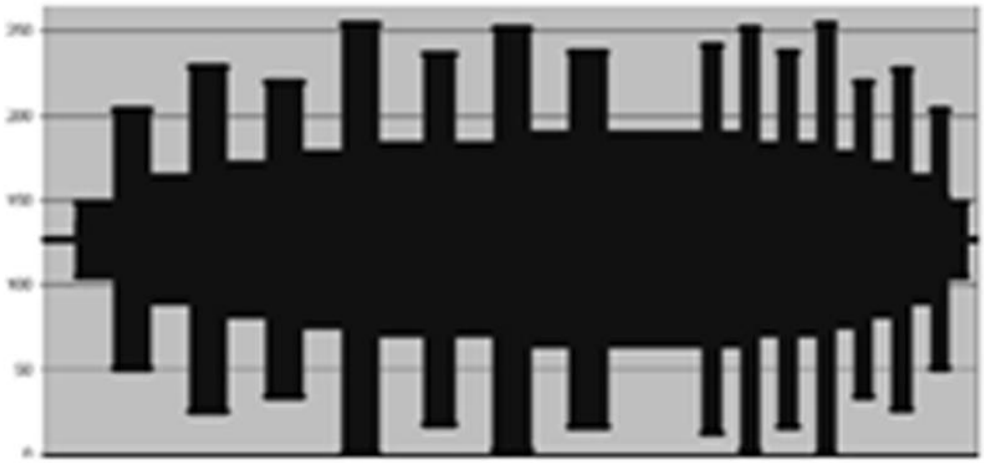

Figure 1. Waveform image of GMA-patterned field repeated over the course of each exposure; the y-axis is waveform point value (equivalent to voltage value between -5 to +5 V), the x-axis is time

Actual geomagnetic activity before, during, and after testing was examined using estimated 3-hour Kp-indices obtained from the Solen database (www.solen.info/solar/).

Random data was produced using a Psyleron REG-1 random event generator (Figure 2; www.psyleron.com). The device produced a random output which was generated by electron tunneling effects within two field effect transistors. The varying voltage levels which result from this process were converted into digital data through a gated sampling procedure which allowed for regularly spaced bit sequences. The output of both transistors was internally compared through an alternating (0, 1) XOR masking process in order to reduce any potential influence of physical artifacts or other external environmental variables. The device itself was further protected from static electromagnetic factors by an aluminum outer shielding and a Permalloy mu-metal inner shield. Furthermore, the device was rigorously calibrated prior to shipment in order to ensure output conformed to statistical expectations.

The random event generator (REG) was also tested in control experiments within our laboratory to confirm these expectations. The resulting data stream is collected through USB-port using Psyleron FieldREG and Reflector software packages on a laptop computer. Individual events were produced at a rate of either 4/sec for larger samples, or 1/sec for shorter samples in order to accommodate participant availability (~5 and 2 minutes per condition respectively). However, internal consistency was maintained across all conditions; for a given participant, each condition was run using the same event rates and test time. There were no significant differences noted between event rates in this experiment or others ($p > .05$). Values for each event refer to the number of 1's out of 200 bits with binary probabilities, represented by a value of 0-200. The theoretical (chance) mean for each event is 100 with a standard deviation of $\sqrt{50}$.

Measures of entropy (HX) were obtained using Matlab 2011a software. All other statistical procedures were conducted using SPSS software v.17.

Figure 2. Random event generator (REG); Psyleron REG-1 device used throughout the following experiment

2.3. Procedure

Each participant was seated in a comfortable chair located within an acoustic chamber which was also a Faraday cage. The large coils were placed on either side of the participant at a distance of ~36 cm (Figure 3). The REG device, also within the coils, was placed ~25 cm from the right side of the participant (Figure 4). Each individual was asked to intend for a specific outcome in the REG data (e.g., Figure 5). All participants completed four conditions, presented in a rotating A-B-C-D order (e.g., presentation order for the first participant was A-B-C-D, second participant was B-C-D-A, etc.). The REG continuously collected data throughout the experiment. The first condition consisted of a relaxed state with no current from the coils (Baseline-No Field). The second condition maintained the relaxation state while the EMF was applied (Baseline-Field). The third consisted of the participant intending on the REG output with the coils again producing no current (Intention-No Field), while the final condition involved another intention task during simulation of EMF increase (Intention-Field).

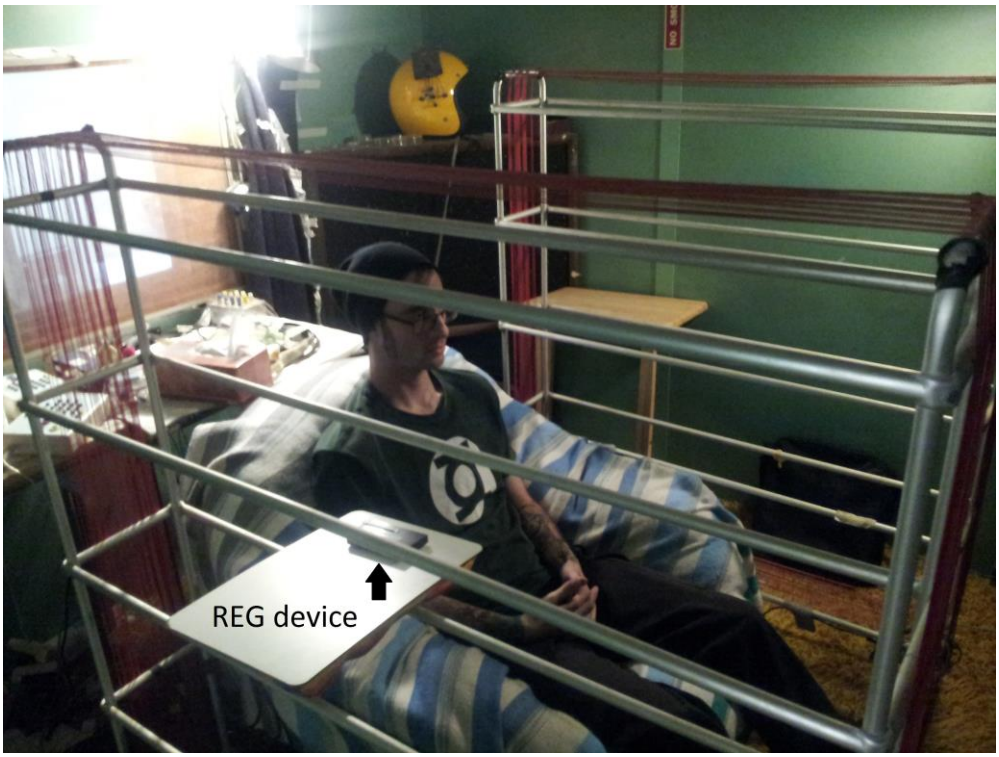

Figure 3. Custom-built coils placed 1 m apart on either side of participant

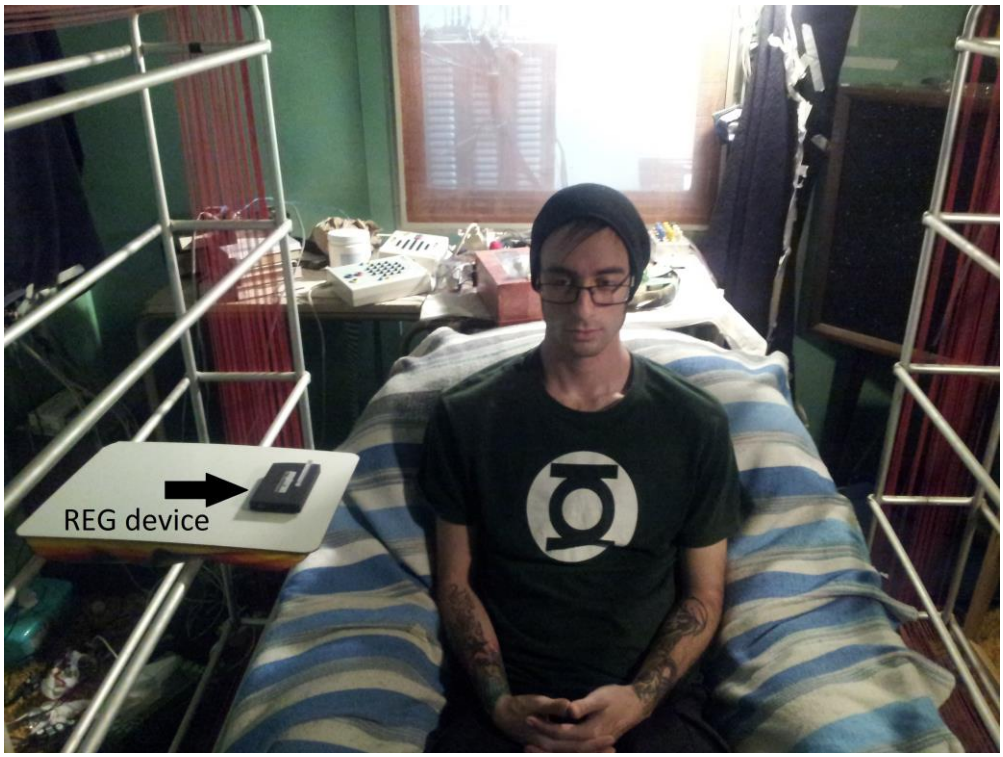

Figure 4. EMF coils on either side of participant, REG device placed on right side within field

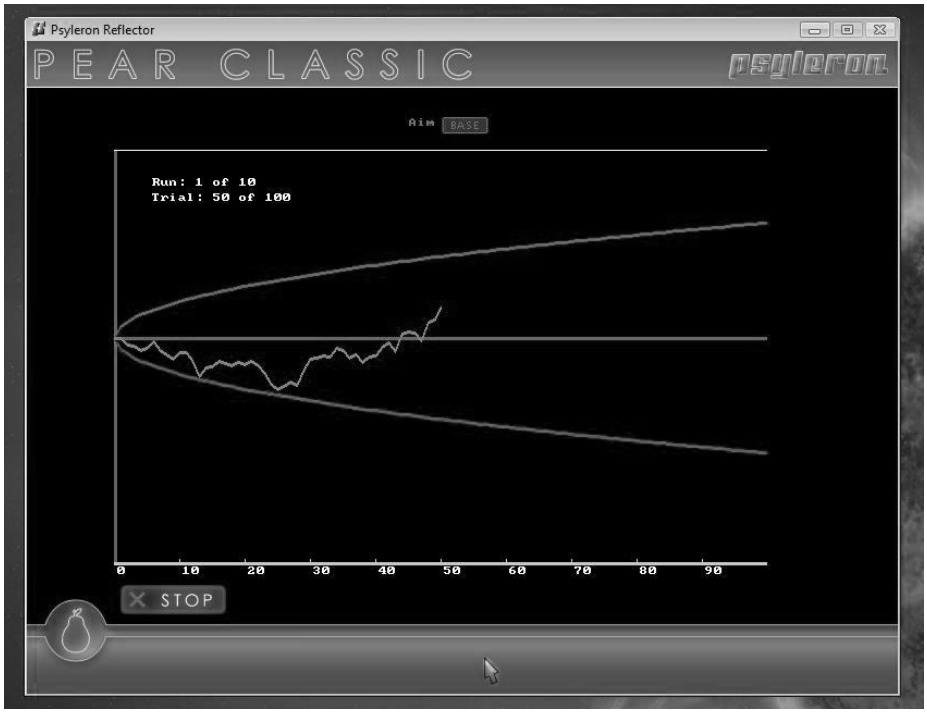

Figure 5. Screenshot of Reflector software collecting data from REG device; jagged center line is the moving cumulative deviation

3. Results

3.1. Data Transformation

REG data was converted where operator intention was present so that the data were maintained, but the overall deviation was reversed in order to represent the direction of intention. Positive deviations indicate the direction intended for, negative scores indicate deviations in the opposite direction of operator intention. Where necessary, data reversal was accomplished by obtaining the absolute deviation of each event (x-100) and multiplying the product by -1 before re-adding 100 (e.g., 105 = 105-100 = 5, 5 · -1 = -5, -5+100 = 95). Following relevant transformation, event data were standardized according to 0.5 chance expectations ([x-100] / √50).

3.2. Simulated Electromagnetic Increases and Operator Performance

In order to account for varied event samples, z-scores for each condition were obtained (Table 1) by computing the deviation from the chance value mean ($\delta_\mu = \mu_{\text{event scores}} - 100$), as well as the measurement uncertainty associated with δ_μ ($\sigma_\mu = \sigma / \sqrt{N}$, where $\sigma = \sqrt{50}$). Dividing these values resulted in a combined z-score for each condition used to obtain subsequent probabilities ($z_c = \delta_\mu / \sigma_\mu$). It was determined that none of the conditions presented with statistically significant overall deviations ($p > .05$), with the possible exception of the Intention-No Field condition, which was marginally significant given one-tailed probabilities ($z_c = 1.84$, $p = .033$). However, the Baseline-Field condition revealed somewhat suggestive results, approaching statistical significance (z_c = -

1.755, p = .08), particularly given the two-tailed probability typically assigned to REG experiments where no specifically intended outcome is present. Furthermore, the Intention-Field condition showed low numbers of overall deviations in the direction intended by the operator (~17%; Figure 6), particularly compared to previous experiments where this ratio tended towards ~50-90% or greater. Similar values were computed for all relevant condition pairings (Table 2) in order to determine which conditions were significantly different from one another. Combined z-scores indicated the only difference which was marginally significant was between Intention-No Field and Intention-Field conditions (z_c = 1.827, p = .034), suggesting that sudden increases in EMF may inhibit initiation of a non-local 3C interaction. Furthermore, increased EMF may actually distort the effects of 3C by encouraging deviations opposite to those intended.

Table 1. Detailed REG results for overall conditions (Baseline-No Field, Baseline-Field, Intention-No Field, Intention-Field, data converted to directional measures (e.g., accounting for intended direction of deviations)

Parameter	BL (No Field)	BL (Field)	Int (No Field)	Int (Field)
N	5565	5669	5657	5641
$\boldsymbol{\mu}$	100.043	99.835	100.173	99.93
sd	6.951	7.109	7.148	7.161
$\boldsymbol{\sigma_{sd}}$	.067	.066	.066	.067
$\boldsymbol{\delta_{\mu}}$	.043	-.165	.173	-.07
$\boldsymbol{\sigma_{\mu}}$	.095	.094	.094	.094
$\boldsymbol{z_c}$	.453	-1.755	1.84	-.745
p	.65 **	.08 **	.033 *	.228 *
%ID	.75 †	.125 †	.5	.167

Parameter Key:
N: Number of events (200 bits/event)
$\boldsymbol{\mu}$: Mean event score (0-200)
sd: Standard deviation of REG event scores
$\boldsymbol{\sigma_{sd}}$: Measurement uncertainty in value of sd; $\sigma_{sd} = \sigma / \sqrt{2N}$, where $\sigma = \sqrt{50}$
$\boldsymbol{\delta_{\mu}}$: Absolute deviation from theoretical chance expectations (μ-100)
$\boldsymbol{\sigma_{\mu}}$: Measurement uncertainty in value of δ_{μ}; $\sigma_{\mu} = \sigma / \sqrt{N}$, where $\sigma = \sqrt{50}$
$\boldsymbol{z_c}$: Overall condition z-score adjusted for measurement uncertainty; $z_c = \delta_{\mu} / \sigma_{\mu}$
p: Probability of z_c * & **
%ID: Proportion of sessions with deviation in the intended direction; *%ID* = N*s* $_{\text{with intention}}$ / N*s*, where N*s* = number of test sessions †

†For directionality of baseline sessions, positive values are considered to be with intention.
*One-tailed probability (e.g., intention involved).
**Two-tailed probability (e.g., no intention).

Table 2. Detailed REG results comparing overall Intention (Int) conditions with respective Baseline (BL) conditions and each other, data converted to directional measures (e.g., accounting for intended direction of deviations)

Parameter	Int (No Field)-BL	Int (Field)-BL	Int No Field-Field
N	11222	11310	11298
δ_μ	.13	.095	.243
σ_μ	.134	.133	.133
z_c	.97	.714	1.827
p	.166 *	.238 *	.034 ****

Parameter Key:
N: Combined number of events (200 bits/event)
δ_μ: Absolute deviation; e.g., = $\mu_{\text{intention}} - \mu_{\text{baseline}}$
σ_μ: Measurement uncertainty in δ_μ; e.g., $\sigma \cdot \sqrt{([1 / N_{\text{intention}}] + [1 / N_{\text{baseline}}])}$, where $\sigma = \sqrt{50}$
z_c: z-score of overall difference adjusted for measurement uncertainty; $z_c = \delta_\mu / \sigma_\mu$
p: Probability of z_c (one-tailed)

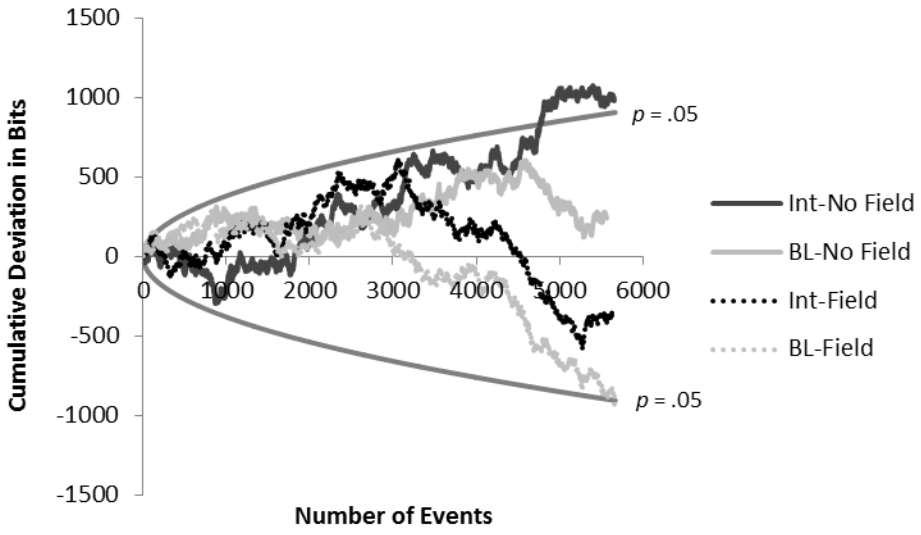

Figure 6. Cumulative deviations from the mean for REG data combined from each condition (Intention-No Field, Baseline-No Field, Intention-Field, Baseline-Field); parabolas indicate threshold for statistical significance (p = .05, one-tailed)

Although the traditional method for presenting deviations in REG experiments have been to cumulate the deviations over successive subjects (Figure 6), this approach does not reveal the actual change in time. To reveal this effect, the mean variations in bits per 10 s increment were completed for the subjects in the four conditions as a function of 10 s increments. The means and standard errors are shown in Figure 7. Two way analysis of variance with one between (treatment) and one within (10 s increments) revealed statistically significant interactions

between the four treatments and the temporal increments ($F_{(3, 31)}$ = 4.333, p = .013, η^2 = .317). *Post hoc* analyses indicated that the major significant effect was due to the significant difference between the group intending while the field was being presented compared to the period of no intention with field presentation (p = .008) during the second increment (10 to 20 s) after the intention began. In other words, intending during the presence of the magnetic field resulted in numbers of REG events comparable to periods of no intention. This could be interpreted as this field pattern "cancelled" or "nullified" the effect of intention upon the random process.

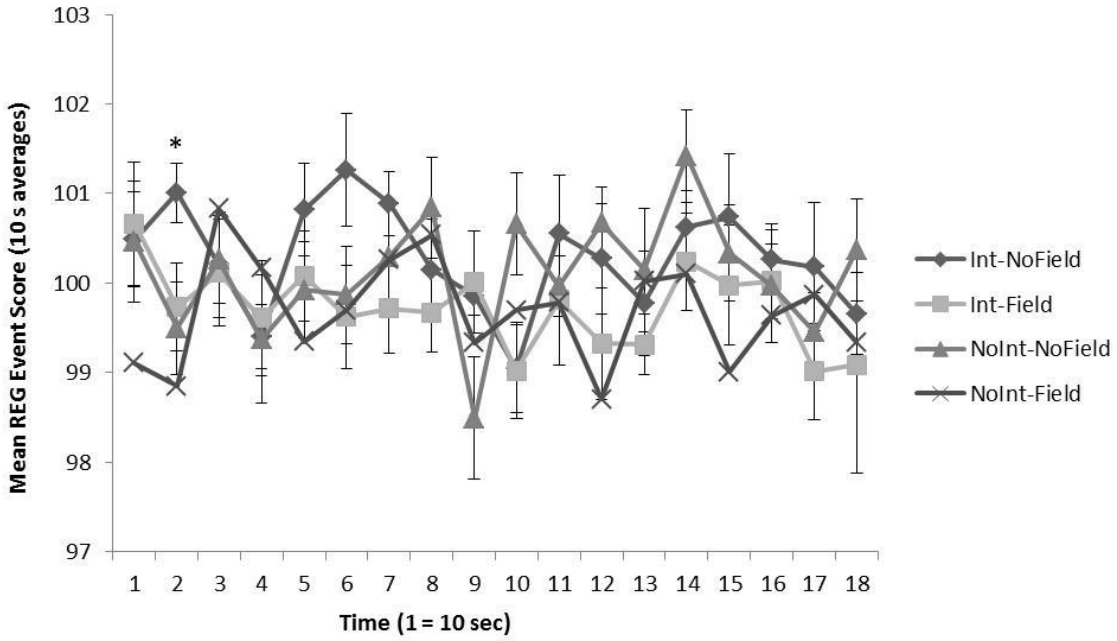

Figure 7. Averaged REG event scores for 10 s increments within each condition; * significant difference between Intention-No Field and Intention-Field conditions (Time 2)

3.3. Electromagnetic Field Increases and REG Complexity

Measures of statistical entropy (HX) were computed for REG data using Matlab software. The measure of entropy computed by this method is similar to Shannon entropy of a random variable [29], $H(X) = -\sum x\ P(x)\log_2 P(x)$, where x = the random variable, X = the number of possible values within x, and P = the probability mass function. Entropy values (HX) represent the level of uncertainty within the data, where higher values indicate greater complexity and less predictability. Signals with greater complexity possess a greater number of distinct values, and these values are more evenly distributed.

A one-way ANOVA was used to demonstrate a statistically significant difference in REG complexity between conditions (Figure 8; $F_{(3, 31)}$ = 5.308, p = .005, η^2 = .362). Post-hoc tests (Tukey) revealed a difference closely approaching statistical significance between Baseline-No Field and Baseline-Field conditions (p = .05). Similar results were also obtained for the difference between Intention-No Field and Intention-Field conditions (p = .05). However, a significant difference was much more apparent for that observed between Baseline-No Field and Intention-Field conditions (p = .009). These results might suggest that sudden electromagnetic

increases may tend to decrease the overall complexity of subsequent REG output, regardless of any apparent 3C interaction.

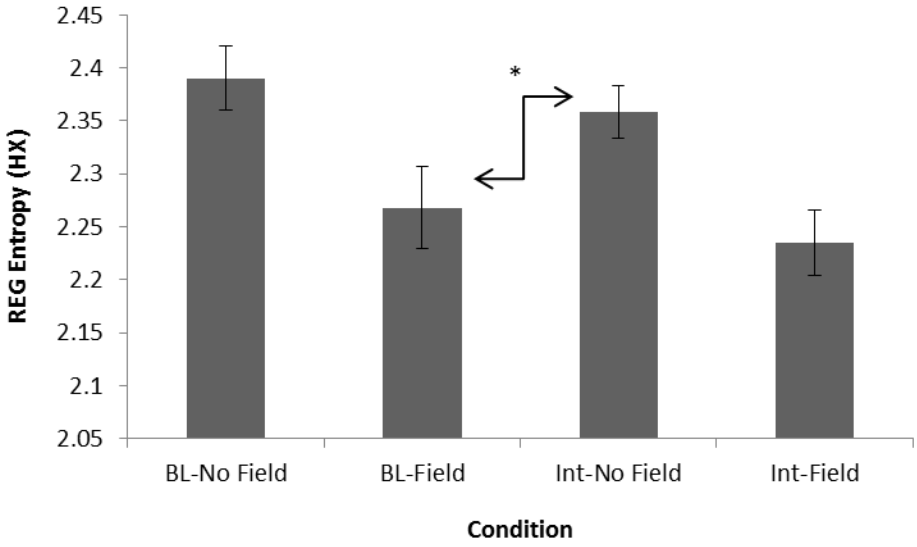

Figure 8. Mean REG entropy (HX) for each condition (Baseline-No Field, Baseline-Field, Intention-No Field, Intention-Field); vertical bars represent SEM; * indicates difference is non-significant ($p > .05$)

3.4. Controlling for Actual Geomagnetic Activity

In order to determine if any potential interaction was present between the use of simulated EMF increases and actual GMA, estimated Kp-indices were obtained for the two 3-hour periods prior to each test session, as well as the Kp-index during testing. A series of ANCOVAs were performed to investigate any potential differences in both REG z-score (Stouffer's method = $\sum z / \sqrt{n}$) and REG entropy (HX) between conditions while controlling for the effects of the actual geomagnetic field. Statistically significant differences between conditions were observed for both REG variables (HX and overall z-score) when covarying for all Kp values (Figure 9; $p < .05$). Furthermore, the effect sizes remained within the same range as that found in the original analysis (η^2s = ~36%).

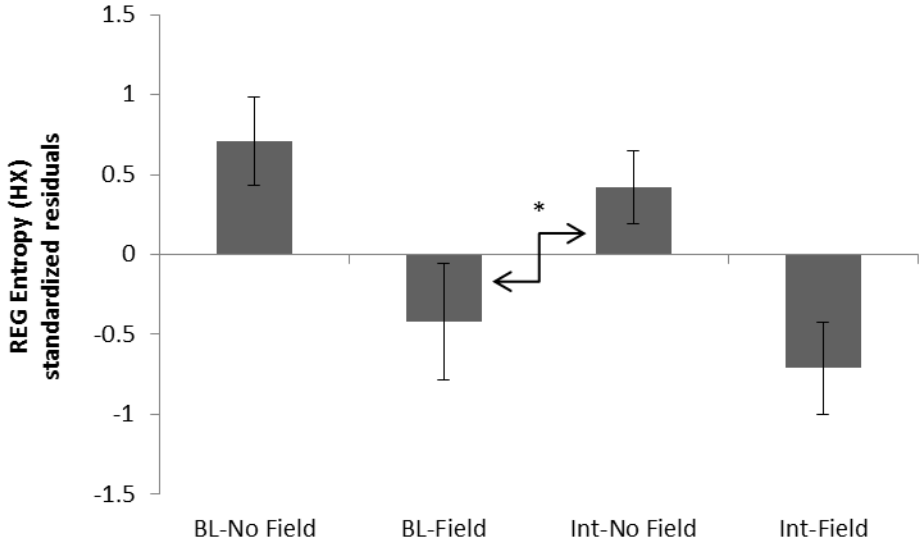

Figure 9. Mean REG entropy (HX) residuals (covarying for Kp-index) for each condition (Baseline-No Field, Baseline-Field, Intention-No Field, Intention-Field); vertical bars represent SEM; * indicates difference is non-significant ($p > .05$)

4. Discussion

The results of these experiments suggest that random variations produced by electron tunneling through commercial devices (Random Event Generators) can be affected by intention. The traditional critique of these reliable although weak effects is that simply the proximity of the human mass, associated within the order of 100 $W \cdot m^{-2}$ of power output, might be mediating these subtle effects. In the present experiments (Figure 6) intention was associated with a significant deviation from "random variation". However application of this patterned magnetic field to the whole body cancelled this effect and evoked changes in the opposite direction. Without intention, that is when the person was still sitting in the same place in order to control for body mass (presence) effects and not intending, the random variations during both the presence and absence of the field was remarkably similar.

"Cancellation" or "reversal" of effects from a competitive agonist in neuropharmacology is well known. Usually this is associated with the remarkably similar molecular structure of the competitive structure with the natural agonist. Mach and Persinger [30] reported similar effects following whole body exposure of rats to a pulsed magnetic field. It was the same temporal structure that when applied as electric currents to hippocampal slices produced Long Term Potentiation (LTP) which is the electromagnetic-chemical substrate for the representation of experience (memory) within the mammalian brain. Mach and Persinger [30] found that the LTP pattern presented as a magnetic field to the animal *before* periods of repeated training in a spatial memory task markedly inhibited the learning. The same pattern presented after the hourly learning trials did not affect learning. The powerful effect from these weak (1 μT, 1000

nT) magnetic fields applied to the whole body, were comparable to that of complete saturation of the hippocampal fields by direct current induction.

In the present study the "reversal" of the intention effect which is clearly seen in Figure 6 occurred when the subjects were exposed to 400 to 500 nT (peak) intensity magnetic fields generated through a series of 3 ms point durations. Because simply the presence of the person *without intention* did not affect the random variations nor did the application of the magnetic fields significantly affect the changes, we assumed that cerebral processes were the mediating factor. The amount of energy from the applied field within the human cerebrum can be calculated by $E=[B^2 \cdot (2\mu)^{-1}] \cdot m^3$, where B is the field strength, μ is magnetic permeability and m is the volume. Assume a volume of the cerebral cortices to be ~0.57 10^{-3} m^3 (570 cc) the energy would be $0.5 \cdot 10^{-11}$ J. If the intrinsic frequency associated with the repeated pattern (~16 s) or $6.3 \cdot 10^{-2}$ Hz is considered the power is $3.2 \cdot 10^{-13}$ J per s.

For comparison the energy-mass equivalence of an electron is $9.1 \cdot 10^{-31}$ kg $\cdot 9 \cdot 10^{16}$ $m^2 s^{-2}$ or $0.8 \cdot 10^{-13}$ J. These two quantities of energy are within the same order of magnitude and would converge when the lower end of the applied magnetic field strengths was involved. Although the concept that magnetic energy within a cerebral volume from an applied field could be converted to and equivalent mass may not be conventional, there are theoretical arguments. First one of the assumptions of the Casimir effect is that virtual particles within the Zero Point Potential Vacuum can be converted to actual particles by electromagnetic fields with changing boundaries. The spatial variations in our time-varying magnetic fields could meet this criterion.

In addition, as calculated by Persinger et al [24] the discrepancy in velocity to produce the differential width of a classical electron (~10^{-15} m) and that calculated as the Compton wavelength based upon energy (~10^{-12} m) would also produce a differential energy-equivalence for an electron mass moving at these two velocities. The discrepancy is 10^{-20} J which is the amount of energy associated with a single action potential. Stated alternatively, the "collapse" of the wave to produce a particle would be associated with an increment of energy associated with the act of thinking. Hence there is both a theoretical basis and quantitative convergence to support the possibility that magnetic energy within cerebral mass could result in the "formation" of an electron or at least its virtual manifestation for a brief period.

At the distance of the REG unit, about 25 cm or 30 cm from the center of the cerebrum, the area of the sphere produced by this radius is ~1.1 m^2. Hence the power density from the energy induced by the applied magnetic field in the cerebral volume if radiated equally in all directions would be ~$3 \cdot 10^{-13}$ $W \cdot m^{-2}$. Assuming the width of the p-n junction was similar to other semiconductor devices, or 10^{-12} m^2, the energy per second would be $3 \cdot 10^{-25}$ J. Although possibly spurious we suggest that the resulting frequency, obtained by dividing by Planck's constant of $6.626 \cdot 10^{-34}$ J·s, which is within range of the neutral hydrogen line (1.42 GHz, 21.1 cm) could be relevant to the phenomena. One could argue that access to this line, given its prominence throughout the known universe, allows access to the most intrinsic properties of the entire universe within a specific location.

The origin of the neutral hydrogen line becomes relevant to the quantities we measured. According to quantum interpretations, when the spins of the proton and electron are in the same direction the magnetic interactions exhibit more energy than if the two particles are spinning in opposite directions. The transition between these two states is associated with the hydrogen line. Although the transition is infrequent, that is only about 10^{-15} per s for one atom or a transition once every 10 million years, the large numbers of this elementary pair (a proton and electron) minimizes this constraint. For example, assuming a brain mass of 1.5 kg and the mass of a proton, there would be ~10^{27} proton equivalents within the human cerebrum. Because of the approaching neutrality of this mass, there would be a comparable number of electrons but these masses would be, in comparison, negligible.

This would allow 10^{12} of those "hypothetical pairs" to generate the transition energy per second. Given the quantum energy of 1.42 GHz (multiplied by Planck's constant) is $9.41 \cdot 10^{-25}$ J, this number of shifts per second within the brain volume would result in available energy of ~10^{-12} J per s or 10^{-12} W. With a total cortical surface area in the order of 10^{-1} m^2 the approximate power density would be ~10^{-11} W $\cdot m^{-2}$. This value is within the order of magnitude of measured photon emissions from the cerebrum during periods of focused cognition, such as imagining white light [31]. However all of the proton-electron pairs within the brain mass are not arranged as neutral hydrogen so this convergence may be coincidental unless there is some recondite geometry or structure that maintains the functional equivalence of this effect.

The absolute differences in the numbers of bits that deviated during intention and when the magnetic field was present during intention were about 3000. Adjusting for the total duration of the exposures for the subjects (about 1440 s), this would be associated with the energy of about 2 electron mass equivalents per second. This number is within the order of magnitude predicted by the energy produced within the brain per second. Even if we accommodated the variability of the intensity of the applied field and the individual differences for the time required to produce the significant deviations from chance, the similarity of values indicate a potential quantitative support for this process.

Why a quantum of energy within the cerebrum would affect specifically the quantum of energy that simulates the movement of an electron across a p-n junction, in our opinion, is by far a more important question. If *non-locality* is operative, then the conditions within the cerebrum and the REG should be similar. The geometry may not be identical to the conditions by which photon "entanglement" has been shown experimentally by Dotta and Persinger [32] and may involve a fundamental form of entanglement that originated from primordial spin processes with direct relevance to consciousness [33]. In the Dotta and Persinger studies [32] simultaneous injection of hydrogen peroxide into sodium hypochlorite in two separated localities produced a doubling of the photon emissions (measured by photomultiplier tubes), as if the two localities were the "same space", at least transiently, or that had been a transposition of three-dimensional spatial axes. However, this only occurred if both localities shared the same space-time structural features of the rotating magnetic fields with specific changes in angular velocities.

We suggest that the capacity for "excess correlation" between intention of the participant and the shift in random variations of electron tunnelling within the REG is related to the shared similarities of their geometries and spaces within which the dynamics occur. In general, the widths of the p-region and n-region in a semiconductor are about $1.5 \cdot 10^{-7}$ m and $2.9 \cdot 10^{-7}$ m, respectively. The total depletion width is about $0.4 \cdot 10^{-6}$ m. This width is within the range of the synapse (contact diameter=0.5 to $2 \cdot 10^{-6}$ m). The tunnelling of electrons occurs within barriers of thickness around 1 to 3 nm (or smaller) while the typical separation of the pre- and post-synaptic cleft or distance for (chemical synapses) is about 20 to 40 nm and electrical "synapses" or gap junctions are about 2 to 3.5 nm. The gap for electron tunneling in a typical device can be obtained by combining the widths of the p- and n-regions ($1.5 \cdot 10^{-7}$ m and $2.9 \cdot 10^{-7}$ m respectively). The ratio of the gap for electron tunnelling to the width through a semiconductor medium would be $2 \cdot 10^{-9}$ m divided by $4.4 \cdot 10^{-7}$ m or $0.45 \cdot 10^{-2}$. The ratio of the gap to width for the chemical synapse would be $3 \cdot 10^{-8}$ m divided by $1.3 \cdot 10^{-6}$ m or $2.3 \cdot 10^{-2}$. In comparison, the ratio of the gap to width of the gap junction involves $3 \cdot 10^{-9}$ dived by $1.3 \cdot 10^{-6}$ m or $0.24 \cdot 10^{-2}$. Considering the range involved for both p-n junctions and electrical (gap junction) synapses, the ratios of gap to width values for both of these conditions are remarkably similar.

Electrical interfaces within the brain are as numerous as chemical synapses within the cerebral cortices, thalamus, and hippocampus. Gap junctions are actual physical connections that couple neighbouring neurons by large macromolecules that traverse the membranes of both adjacent neurons. Direct exchange of ions and smaller molecules occur between the two cells. Gap junctions are known for their capacities to rectify (facilitate current in one direction rather than another) movements of charges as well as to coordinate electrical changes within large populations of neurons. They couple with GABAergic interneurons within cerebral cortices and thalamus, particularly in young animals. Spike transients from action potentials can penetrate the gap junction and synchronize multiple neurons that share these interfaces including distributed neuronal circuits [34].

This results in the synchronization of the "40 Hz" cortical rhythms which is minimized if the expression of the chemical substrates for the gap junction is prevented because of an absent gene. Gap junctions are also likely to be responsible for the revealing 40 Hz cortical patterns that are commonly seen superimposed upon the theta (4 to 8 Hz) synchronous patterns generated by the hippocampal formation. Such electrical coupling over large area and volumes of cerebral cortical space may be the "cohesive" factor that has been considered essential for producing a "cognitive field" as well as increasing the total power output by summating the very small quantities that would otherwise be cancelled into an integrated value of substantial magnitude.

There may be quantitative suggestions for the potential entanglement of energy and mass between the gap junctions within the participants' cerebral cortices and hippocampal formations and the p-n junctions of the REG at approximately 0.25 m distance. If we assume a classic Casimir effect described by:

$$[\pi^2 (240)^{-1} \hbar c a^{-4}] \cdot S \quad (1),$$

where ħ is the modified Planck's constant, c is the velocity of light and a is the distance between the two planes (2 nm) with surface area S of 0.16 μm^2 , the force would be $0.13 \cdot 10^{-4}$ N and when applied across the 2 nm interface would involve an energy of $0.26 \cdot 10^{-13}$ J. The mass equivalent of that energy is within range, given the variation in width and separation distances for both gap and p-n junctions to that of the classical electron ($\sim 10^{-31}$ kg). One of the basic assumptions for the Casimir force is that virtual particles can become actual particles when the appropriately time-varying magnetic field is applied to a changing boundary. The time-varying magnetic field employed in our present study could meet the criteria for that condition.

On the other hand, the complexity of the digital sequences generated by the REG was not affected by intention. There was a general decrease in complexity when the experimental field was applied, regardless if intention was present or absent. A decrease in complexity could be associated with the consequence of repeating the same field pattern which by definition would have deviated from the greater degrees of freedom that would constitute complexity. The etiology of this effect is not clear. It is not likely to be related to crude current induction because other experiments in which the field strengths were altered did not change the degree of complexity. From another perspective, the fact that the actual deviation of the REG output was affected by intention and attenuated by the simultaneous application of the magnetic field, whereas complexity was not affected by intention, indicates that the two phenomena are quite separate. In addition this differential indicates that the effects of intention involved processes other than non-specific (generalized or artifactual) factors.

References

1) Mouritsen, H., Feenders, G., Liedvogel, M., & Kropp, W. *Migratory birds use head scans to detect the direction of the Earth's magnetic field*. Current Biology, 2004; 14(21): 194+6-1949.

2) Klimley, A. P. *Highly directional swimming by scalloped hammerhead sharks, Sphyrna lewini, and subsurface irradiance, temperature, bathymetry, and geomagnetic field*. Marine Biology, 1993; 117: 1-22.

3) Kimchi, T., Etienne, A. S., & Terkel, J. *A subterranean mammal uses the magnetic compass for path integration*. Proceedings of the National Academy of Sciences of the United States of America, 2004; 101(4): 1105-1109.

4) Dimitrova, S., Mustafa, F. R., Stoilova, I., Babayev, E. S., & Kazimov, E. A. *Possible influence of solar extreme events and related geomagnetic disturbances on human cardio-vascular state: Results of collaborative Bulgarian-Azerbaijani studies*. Advances in Space Research, 2009; 43(4): 641-648.

5) Mulligan, B. P., Hunter, M. D., & Persinger, M. A. *Effects of geomagnetic activity and atmospheric power variations on quantitative measures of brain activity: Replication of the Azerbaijani studies*. Advances in Space Research, 2010; 45(7): 940-948.

6) Babayev, E. S., & Allahverdiyeva, A. A. *Effects of geomagnetic activity variations on the physiological and psychological state of functionally healthy humans: Some results of Azerbaijani studies*. Advances in Space Research, 2007; 40(12): 1941-1951.

7) Snyder, C. W., Neugebauer, M., & Rao, U. R. *The solar wind velocity and its correlation with cosmic-ray variations and with solar and geomagnetic activity*. Journal of Geophysical Research, 1963; 68(24): 6361-6370.

8) Persinger, M. A. *The possible role of dynamic pressure from the interplanetary magnetic field on global warming*. International Journal of Physical Sciences, 2009; 4(1): 44-46.

9) Richardson, I. G., Cliver, E. W., & Cane, H. V. *Sources of geomagnetic storms for solar minimum and maximum conditions during 1972-2000*. Geophysical Research Letters, 2001; 28(13): 2569-2572.

10) Jahn, R. G., Dunne, B. J., Nelson, R. D., Dobyns, Y. H., & Bradish, G. J. *Correlations of random binary sequences with pre-stated operator intention: A review of a 12-year program*. Journal of Scientific Exploration, 1997; 11(3): 345-367.

11) Radin, D. I., & Nelson, R. D. *Meta-analysis of mind-matter interaction experiments: 1959-2000*. In Healing, Intention, and Energy Medicine (pp. 39-48). London: Harcourt Health Sciences, 2003.

12) Giroldini, W. *Eccles's model of mind-brain interaction and psychokinesis: A preliminary study*. Journal of Scientific Exploration, 1991; 5(2): 145-161.

13) Caswell, J. M., Collins, M. W. G., Vares, D. A. E., Juden-Kelly, L. M., & Persinger, M. A. *Gravitational and experimental electromagnetic contributions to cerebral effects upon deviations from random number variations generated by electron tunneling*. International Letters of Chemistry, Physics and Astronomy, 2013; 11: 72-85.

14) Caswell, J. M., Dotta, B. T., & Persinger, M. A. *Cerebral biophoton emission as a potential factor in non-local human machine interaction*. NeuroQuantology; in press.

15) Makarec, K., & Persinger, M. A. *Geophysical variables and behavior: XLIII. Negative correlation between accuracy of card-guessing and geomagnetic activity: A case study*. Perceptual and Motor Skills, 1987; 65: 105-106.

16) Krippner, S., & Persinger, M. A. *Evidence for enhanced congruence between dreams and distant target material during periods of decreased geomagnetic activity*. Journal of Scientific Exploration, 1996; 10(4): 487-493.

17) Dotta, B. T., & Persinger, M. A. *Dreams, time distortion, and the experience of future events: A relativistic, neuroquantal perspective*. Sleep and Hypnosis, 2009; 11(2): 29-39.

18) Hunter, M. D., Mulligan, B. P., Dotta, B. T., Saroka, K. S., Lavallee, C. F., Koren, S. A., & Persinger, M. A. *Cerebral dynamics and discrete energy changes in the personal environment during intuitive-like states and perceptions*. Journal of Consciousness Exploration & Research, 2010; 1(9): 1179-1197.

19) Persinger, M. A., Dotta, B. T., Saroka, K. S., & Scott, M. A. *Congruence of energies for cerebral photon emissions, quantitative EEG activities and ~5 nT changes in the proximal geomagnetic field support spin-based hypothesis of consciousness*. Journal of Consciousness Exploration & Research, 2013; 4(1): 1-24.

20) Gissurarson, L. R. *The psychokinesis effect: Geomagnetic influence, age and sex differences*. Journal of Scientific Exploration, 1992; 6(2): 157-165.

21) Radin, D. I. *Environmental modulation and statistical equilibrium in mind-matter interaction.* Subtle Energies, 1993; 4(1): 1-30.

22) Gearhart, L., & Persinger, M. A. *Geophysical variables and behavior: XXXIII. Onsets of historical and contemporary poltergeist episodes occurred with sudden increases in geomagnetic activity*. Perceptual and Motor Skills, 1986; 62: 463-466.

23) Roll, W. G., Saroka, K. S., Mulligan, B. P., Hunter, M. D., Dotta, B. T., & Gang, N. *Case report: A prototypical experience of 'poltergeist' activity, conspicuous quantitative electroencephalographic patterns, and sLORETA profiles: Suggestions for intervention*. Neurocase: The Neural Basis of Cognition, 2012; 18(6): 527-536.

24) Persinger, M. A., Koren, S. A., & Lafreniere, G. F. *A neuroquantologic approach to how human thought might affect the universe*. NeuroQuantology, 2008; 6(3): 262-271.

25) Persinger, M. A. *Solutions for real values of Minkowski four-dimensional space may link macro- and micro-quantum processes in the brain*. Neuroscience and Biobehavioral Reviews, 2012; 36: 2334-2338.

26) Saroka, K. S., Caswell, J. M., Lapointe, A., & Persinger, M. A. *Greater electroencephalographic coherence between left and right temporal lobe structures during increased geomagnetic activity*. Neuroscience Letters, 2013; 560, 126-130.

27) Mulligan, B. P., & Persinger, M. A. *Experimental simulation of the effects of sudden increases in geomagnetic activity upon quantitative measures of human brain activity: Validation of correlational studies*. Neuroscience Letters, 2012; 516(1): 54-56.

28) Murugan, N. J., Karbowski, L. M., Lafrenie, R. M., & Persinger, M. A. *Temporally-patterned magnetic fields induce complete fragmentation in planaria*. PLoS ONE, 2013; 8(4).

29) Shannon, C. E. *A mathematical theory of communication*. The Bell System Technical Journal, 1948; 27: 379-423, 623-656.

30) Mach, Q. H., & Persinger, M. A. *Behavioral changes with brief exposures to weak magnetic fields patterned to simulate long-term potentiation*. Brain Research, 2009; 1261, 45-53.

31) Dotta, B. T., Saroka, K. S., & Persinger, M. A. *Increased photon emission from the head while imagining light in the dark is correlated with changes in electroencephalographic power: Support for Bokkon's biophoton hypothesis*. Neuroscience Letters, 2012; 513(2), 151-154.

32) Dotta, B. T., Koren, S. A., & Persinger, M. A. *Demonstration of entanglement of "pure" photon emissions at two locations that share specific configurations of magnetic fields: Implications for translocation of consciousness*. Journal of Consciousness Exploration & Research, 2013; 4(1).

33) Hu, H. & Wu, M. *Spin as primordial self-referential process driving quantum mechanics, spacetime dynamics and consciousness*. NeuroQuantology, 2004; 2(1), 41-49.

34) Traub, R. D., Kopell, N., Bibbig, A., Buhl, E. H., LeBeau, F. E. N., & Whittington, M. A. *Gap junctions between interneuron dendrites can enhance synchrony of gamma oscillations in distributed networks*. Journal of Neuroscience, 2001; 21(23), 9478-9486.